A Tiling-Based Approach for Directional Sensor Network Deployment

Chun-Hsien Wu
Information and Communications Research Laboratories
Industrial Technology Research Institute
Hsinchu, Taiwan, R.O.C.
ChunHsienWu@itri.org.tw

Yeh-Ching Chung
Department of Computer Science
National Tsing Hua University
Hsinchu, Taiwan, R.O.C.
ychung@cs.nthu.edu.tw

Abstract—**In this paper, we propose a tiling-based wireless sensor network (WSN) deployment approach based on the polygon model for sensor nodes with directional sensing areas. In the tiling-based deployment approach, a hexagon tile is first generated from the polygon that represents the sensing area of a given directional sensor. Then, a tiling process is applied to place tiles to the deployment area. Both sensing coverage holes surrounding the boundaries and the obstacles are considered under the proposed approach. To evaluate the proposed deployment approach, we compare its performance with the strip-based deployment pattern approach, which is under the sector model, in terms of the sensing coverage rate and the usage of sensor nodes. The simulation results show that the sensing coverage rate of the proposed deployment approach is higher than that of the strip-based deployment pattern approach for different types of sensor nodes on deployment areas with/without obstacles.**

I. INTRODUCTION

With the growing applications of the wireless sensor networks (WSNs), a WSN deployment approach has to fulfill various requirements, such as keeping the network connected, maximizing the sensing coverage rate, minimizing the usage of sensor nodes, etc. In this paper, we focus on the connected area coverage problem under the deterministic WSN deployment. That is, given some deployable sensor nodes, we want to determine the deployment locations of sensor nodes to achieve maximum sensing coverage of the deployment area and maintain network connectivity among deployed sensor nodes. To address these requirements, a proper modeling of the communication or sensing area of a sensor node is essential. In this paper, we assume that the sensor node used has an omnidirectional antenna and a directional sensor. Therefore, a sensor node has a round shape of communication area and an arbitrary shape of directional sensing area. We use the disk model to represent the communication area of the omnidirectional antenna since it is commonly used in many WSN applications with round shaped communication/sensing areas [1], [3], [5]. However, for directional sensors such as infrared sensor or ultrasonic sensor whose sensing areas are not round shape, it is not suitable to represent these directional sensing areas with the disk model. Some models for the sensing area of a directional sensor were proposed in the literature. In [2], [7], [8], the sector model was proposed for directional sensors whose sensing areas are sector shapes. In [10], we proposed a polygon model, which is a more general model compared with disk model or sector model, to approximate different shapes of sensing areas of directional sensors. In the polygon model, the sensing area modeled is a convex polygon. A convex polygon consists of a list of vertices in polar coordinates that outline the actual sensing area of a sensor node. Each vertex represents the distance and direction to the center of a sensor node.

In this paper, we use the polygon model to represent the sensing area of a directional sensor. Based on the polygon model, we propose a tiling-based approach for WSN deployment. A *tiling* (or *tessellation*) of the plane is a process that uses a collection of polygons, called *tiles*, to cover the plane without gaps or overlaps [6]. Since it is impossible to tile a plane with congruent copies of convex polygons with 7 or more edges [4], [9], the proposed approach first generates a hexagonal tile that inscribes the sensing area under the polygon model. Then, the deployment area is filled with generated tiles based on the calculated intervals. In order to maintain the network connectivity among sensor nodes, the intervals between tiles are adjustable. Different from the strip-based deployment pattern (SDP) approach under the sector model [7], the proposed approach can deal with the sensing coverage holes surrounding the boundaries and the obstacles by deploying auxiliary tiles.

This research is funded in part by the Ministry of Economic Affairs of the Republic of China under contract MOEA 99-EC-17-A-03-02-0752 and MOEA 96-EC-17-A-04-S1-044.

II. MODELING THE DIRECTIONAL SENSING AREA

The polygon model proposed in [10] is a general model, compared to the sector model, to approximate the directional sensing area of a sensor node. The formal definition of the polygon model is given below:

Definition 1 (polygon model). *Assume that a sensor node S_n is deployed at the origin of the Euclidean plane and the sensing area of S_n is symmetric about the x-axis. The approximated sensing area of S_n under the polygon model, $poly_S(S_n) = (v_{S1}, \ldots, v_{Si}, \ldots, v_{Sm})$, is a polygon with m vertices, where $m \geq 3$ and $1 \leq i \leq m$. The ith vertex of $poly_S(S_n)$, $v_{Si} = (r_{Si}, \theta_{Si})$, is represented in polar coordinates, where r_{Si} is the distance between v_{Si} and the center of S_n, and θ_{Si} is the counterclockwise angle from 0° (the positive x-axis) to v_{Si}.*

An example of using the polygon model to model the raindrop-like sensing area is given in Fig. 1. In Fig. 1a, $poly_S(S_n) = (v_{S1}, \ldots, v_{S8})$ = [(40, 0°), (35, 10°), (30, 15°), (25, 20°), (0, 180°), (25, 340°), (30, 345°), (35, 350°)] is the approximated sensing area of the raindrop-like sensing area under the polygon model and vertex v_{S5} = (0, 180°) is the center of the sensor node.

When a sensor node is deployed to a field, the sensing area covered by the sensor node varies with its deployment location and rotation angle. In order to represent the same $poly_S(S_n)$ with varies angles in a field, we have the following definition.

Definition 2. *Given a sensor node S_n and $poly_S(S_n)$, when S_n is deployed at $loc(S_n)$ and rotated counterclockwise by $\theta_{rot}(S_n)$, the sensing area covered by $poly_S(S_n)$ in a field is defined as*

$Area_S(S_n) = \{loc(S_n), [(r_{S1}, \theta_{S1}+\theta_{rot}(S_n)), \ldots, (r_{Si}, \theta_{Si}+\theta_{rot}(S_n)), \ldots, (r_{Sm}, \theta_{Sm}+\theta_{rot}(S_n))]\}$.

Given the sensor node S_n and its $poly_S(S_n)$ shown in Fig. 1a, if S_n is deployed at location (10, 20) with rotation angle 30°, we have $Area_S(S_n)$ = {(10, 20), [(40, 30°), (35, 40°), (30, 45°), (25, 50°), (0, 230°), (25, 10°), (30, 15°), (35, 20°)]} which is shown in Fig. 1b.

III. THE TILING-BASED WSN DEPLOYMENT UNDER THE POLYGON MODEL

In this paper, we assume that the sensing area under the polygon model is a convex polygon. We also assume that the sensing area of a sensor node is symmetric about the axis passing through the center of the sensor node. The tile used in the proposed tiling-based WSN deployment is defined as follows.

Definition 3. *Given a sensor node S_n and $poly_S(S_n)$, the tile of a $poly_S(S_n)$, $Tile(S_n) = (v_{T1}, \ldots, v_{Ti}, \ldots, v_{Tm})$, is a convex polygon inscribed in $poly_S(S_n)$, where $v_{Ti} = (r_{Ti}, \theta_{Ti})$, $3 \leq m \leq 6$ and $1 \leq i \leq m$.*

For $Tile(S_n)$ with 6 and 5 edges, there exists a pair of parallel opposite edges of equal length. When S_n is deployed at $loc(S_n)$ with angle $\theta_{rot}(S_n)$, the coverage area of $Tile(S_n)$ in a field is defined as

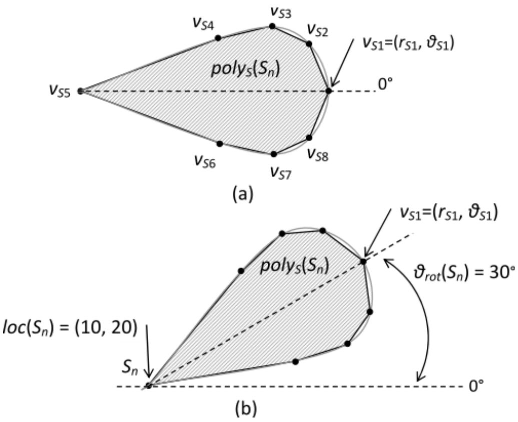

Figure 1. The polygon model: (a) the the raindrop-like sensing area under the polygon model, and (b) a rotated sensing area in a field.

$Area_T(S_n) = \{loc(S_n), [(r_{T1}, \theta_{T1}+\theta_{rot}(S_n)), \ldots, (r_{Ti}, \theta_{Ti}+\theta_{rot}(S_n)), \ldots, (r_{Tm}, \theta_{Tm}+\theta_{rot}(S_n))]\}$.

Since a polygon with less than six vertices can be regarded as a degenerated hexagon, we will focus on the tiling of hexagonal tiles in the rest of the paper. The proposed tiling-based WSN deployment algorithm under the polygon model consists of three phases:

1) Tile generation: In this phase, a hexagonal tile that inscribes the sensing area of a sensor node under the polygon model is generated.

2) Tile placement: In this phase, the deployment area is filled with generated tiles based on the calculated intervals such that the network connectivity among sensor nodes is maintained.

3) Sensing coverage holes reduction: In this phase, the sensing coverage holes surrounding the boundaries and the obstacles are reduced by deploying auxiliary tiles.

The above procedure terminates when either the deployment area is fully covered or no more sensor nodes can be deployed. In the following subsections, we describe each phase in detail.

A. Phase 1: Tile Generation

Given a sensor node S_n with $poly_S(S_n) = (v_{S1}, \ldots, v_{Sc}, \ldots, v_{Sm})$ that is symmetric about the *x*-axis passing through the center of S_n, v_{Sc}, and towards 0°. The generation of a hexagonal $Tile(S_n) = (v_{T1}, \ldots, v_{T6})$ consists of the following steps:

1. Let $v_{T4} = (r_{T4}, \theta_{T4}) = v_{Sc} = (r_{Sc}, \theta_{Sc})$, where $v_{Sc} \in poly_S(S_n)$, $r_{Sc} = 0$ and $\theta_{Sc} = 180°$;
2. Find $v_{T1} = (r_{T1}, \theta_{T1})$ on $poly_S(S_n)$ such that $\theta_{T1} = 0°$ and $r_{T1} = r_S(\theta_{T1})$;
3. Let $\theta_{T3} = \theta_{T4} - 0.1°$;
4. Find $v_{T3} = (r_{T3}, \theta_{T3})$ on $poly_S(S_n)$ such that $r_{T3} = \min(r_S(\theta_{T3}), R_C)$, where R_C is the maximum communication range of S_n;

5. Find v'_{T3} that is the projection of v_{T3} onto x-axis and calculate $d(v_{T3}, v'_{T3})$;
6. Find $v_{T2} = (r_{T2}, \theta_{T2})$ on $poly_S(S_n)$, where $r_{T2} = r_S(\theta_{T2})$, $0° < \theta_{T2} < \theta_{T3}$ and v'_{T2} is the projection of v_{T2} onto x-axis such that $d(v_{T2}, v'_{T2}) = d(v_{T3}, v'_{T3})$;
7. Calculate the area of the trapezoid ⏢$v_{T1}v_{T2}v_{T3}v_{T4}$;
8. Repeat Step 4 to Step 7 by decrementing θ_{T3} by 0.1° until $r_{T3} = R_C$ or no such v_{T2} can be found;
9. Let $v_{T2} = (r_{Tx}, \theta_{Tx})$ and $v_{T3} = (r_{Ty}, \theta_{Ty})$ be the two vertices such that the area of the trapezoid ⏢$v_{T1}v_{T2}v_{T3}v_{T4}$ is the maximum one found in Step 4 to Step 7, where $0° < \theta_{Tx} < \theta_{Ty} < 180°$;
10. Generate another trapezoid ⏢$v_{T1}v_{T6}v_{T5}v_{T4}$ that is the mirror of the trapezoid ⏢$v_{T1}v_{T2}v_{T3}v_{T4}$ symmetric about the x-axis. Then the hexagon generated is $Tile(S_n) = (v_{T1}, v_{T2}, v_{T3}, v_{T4}, v_{T5}, v_{T6})$.

Fig. 2 illustrates how to generate a hexagonal tile from the sensing area under the polygon model shown in Fig. 1a, two trapezoids, ⏢$v_{T1}v_{T2}v_{T3}v_{T4}$ and ⏢$v_{T1}v_{T6}v_{T5}v_{T4}$, are symmetric about the x-axis passing through v_{T1} and v_{T4}.

B. Phase 2: Tile Placement

In this paper, we assume that the deployment area is a rectangular region with or without polygonal obstacles. Once the hexagonal $Tile(S_n)$ is generated in Phase 1, the deployment area can be filled with congruent copies of $Area_T(S_n)$ toward 0° (denoted as *Tile-R*) or 180° (denoted as *Tile-L*) row by row with the following steps:

1. Let the locations of upper-left, upper-right, bottom-left, and bottom-right corners of the deployment area are (0, *width*), (*length*, *width*), (0, 0), and (*length*, 0), respectively;
2. Let $r = 0$, $Tile\_interval\_x = \min(2R_C \times \cos\theta_{T3}, d(v_{T1}, v_{T4}) + d(v_{T2}, v_{T3}))$, $Tile\_offset\_x = r_{T3} \times \cos\theta_{T3}$, and $Tile\_offset\_y = r_{T3} \times \sin\theta_{T3}$;
3. There are i *Tile-R* in Row_{2r} and they are deployed at locations $(d(v_{T2}, v_{T3}), width - 2r \times Tile\_offset\_y)$, $(d(v_{T2}, v_{T3}) + Tile\_interval\_x, width - 2r \times Tile\_offset\_y)$, …, $(d(v_{T2}, v_{T3}) + (i–1) \times Tile\_interval\_x, width - 2r \times Tile\_offset\_y)$, respectively, where $d(v_{T2}, v_{T3}) + (i–1) \times Tile\_interval\_x \leq length < d(v_{T2}, v_{T3}) + i \times Tile\_interval\_x$;
4. There are j *Tile-L* in Row_{2r+1} and they are deployed at locations $(d(v_{T2}, v_{T3}) + Tile\_offset\_x, width - (2r+1) \times Tile\_offset\_y)$, $(d(v_{T2}, v_{T3}) + Tile\_offset\_x + Tile\_interval\_x, width - (2r+1) \times Tile\_offset\_y)$, …, $(d(v_{T2}, v_{T3}) + Tile\_offset\_x + (j–1) \times Tile\_interval\_x, width - (2r+1) \times Tile\_offset\_y)$, respectively, where $d(v_{T2}, v_{T3}) + Tile\_offset\_x + (j–1) \times Tile\_interval\_x \leq length < d(v_{T2}, v_{T3}) + Tile\_offset\_x + j \times Tile\_interval\_x$;
5. Increase r by 1;
6. Repeat Step 3 to Step 5 until either $(width - 2r \times Tile\_offset\_y) < 0$ or $(width - (2r+1) \times Tile\_offset\_y) < 0$.

Fig. 3 shows an example of tiling with the hexagonal tile shown in Fig. 2. In Fig. 3, two sensor nodes with congruent copies of *Tile-R*, $Tile_1$ and $Tile_2$, in Row_0 are deployed at P_1 and P_2, respectively. Similarly, two sensor nodes with congruent copies of *Tile-L*, $Tile_3$ and $Tile_4$, in Row_1 are deployed at P_3 and P_4, respectively. The offsets between P_1 and P_3 in x and y directions are *Tile_offset_x* and *Tile_offset_y*, respectively. To maintain the network connectivity among sensor nodes, if $d(P_2, P_3) > R_C$, the *Tile_interval_x* will be reduced to $2R_C \times \cos\theta_{T3}$ and inducing some overlaps between two adjacent *Tile-R* or *Tile-L* at the same row.

C. Phase 3: Sensing Coverage Holes Reduction

In Phase 2, the generated tiles are deployed in a field based on fixed intervals. As a result, some sensing coverage holes will be surrounding the boundaries and obstacles. An example is given in Fig. 4. In Fig. 4, we observe that the sensing coverage holes surrounding boundaries are caused by unable to deploy sensor nodes outside of the right or lower boundaries of the deployment area. The sensing coverage holes surrounding obstacles are caused by deploying sensor nodes within obstacles. In the following, we will discuss how to reduce the sensing coverage holes surrounding the boundaries and obstacles.

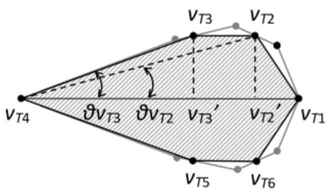

Figure 2. Generates a hexagonal tile.

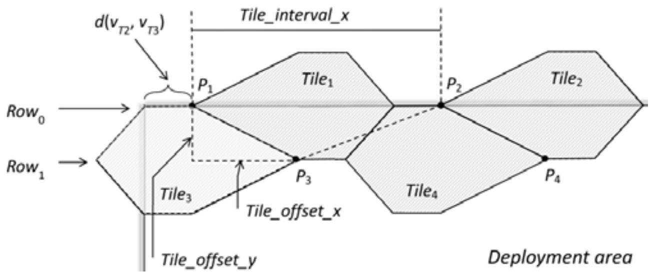

Figure 3. Tiling the deployment area with hexagonal tiles.

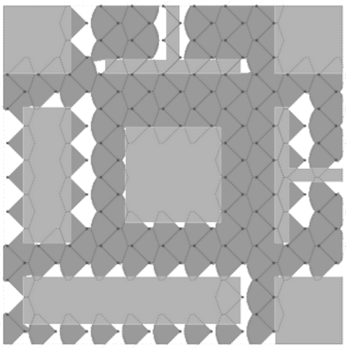

Figure 4. Sensing coverage holes surrounding the boundaries and obstacles.

1) Reduce Sensing Coverage Holes Surrounding the Boundaries

For a sensing coverage hole surrounding the right boundary, it appears at Row_{2r+1}. According to the tile placement process described in Phase 2, there are *j Tile-L* in Row_{2r+1}. The hole is caused by unable to deploy the $(j+1)$th sensor node at location $P_U = (x_U, y_U) = (d(v_{T2}, v_{T3}) + Tile\_offset\_x + j \times Tile\_interval\_x, width - (2r+1) \times Tile\_offset\_y)$. Let $boundary\_dist\_x = x_U - length$ be the distance of P_U to the right boundary. We have the following two cases:

Case 1 ($d(v_{T1}, v_{T4}) > boundary\_dist\_x \geq Tile\_offset\_x$): In this case, the hole surrounding the right boundary will look like the one shown in Fig. 5a. The sensing coverage hole can be fully covered by deploying an auxiliary *Tile-R*, denoted as *Tile-Aux*, at $P_{Aux} = (x_U - 2 \times Tile\_offset\_x - d(v_{T2}, v_{T3}), y_U)$ and the connectivity of the WSN is preserved as shown in Fig. 5b.

Case 2 ($boundary\_dist\_x < Tile\_offset\_x$): In this case, the hole will look like the one shown in Fig. 6a. To fully cover the sensing coverage hole, we need to deploy three auxiliary tiles as shown in Fig. 6b. In Fig. 6b, an auxiliary *Tile-L*, *Tile-Aux*$_1$, is deployed at $P_{Aux1} = (length, y_U)$. Two auxiliary *Tile-R*, *Tile-Aux*$_2$ and *Tile-Aux*$_3$, are deployed at $P_{Aux2} = (length - Tile\_offset\_x, y_U + Tile\_offset\_y)$ and $P_{Aux3} = (length - Tile\_offset\_x, y_U - Tile\_offset\_y)$, respectively. In this way, the sensing coverage hole is fully covered and the connectivity of the WSN is preserved.

For a sensing coverage hole surrounding the lower boundary, we have the following two cases:

Case 3 (The hole appears at Row_{2r}): In his case, the hole is caused by unable to deploy a *Tile-R* at location $P_U = (x_U, y_U) = (d(v_{T2}, v_{T3}) + k \times Tile\_interval\_x, width - 2r \times Tile\_offset\_y)$, where $0 \leq k \leq (i-1)$ and $y_U < 0$. The hole surrounding the lower boundary will look like the one shown in Fig. 7a. Let $boundary\_dist\_y = -y_U$ be the distance of P_U to the lower boundary. We have $boundary\_dist\_y < Tile\_offset\_y$. The sensing coverage hole can be fully covered by deploying an auxiliary *Tile-R* at $P_{Aux} = (x_U, 0)$ and the connectivity of the WSN is preserved as shown in Fig. 7b.

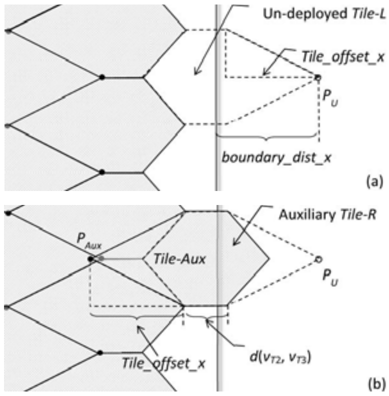

Figure 5. Coverage hole at the right boundary (Case 1): (a) un-deployed *Tile-L* and (b) auxiliary *Tile-R*.

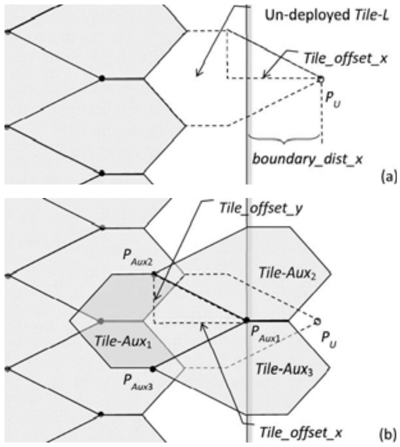

Figure 6. Coverage hole at the right boundary (Case 2): (a) un-deployed *Tile-L* and (b) auxiliary *Tile-R* and *Tile-L*.

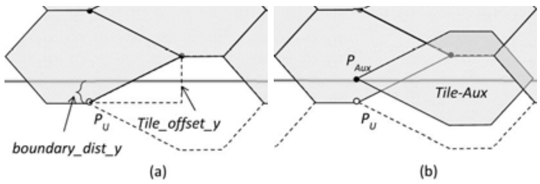

Figure 7. Coverage hole at the lower boundary (Case 3): (a) un-deployed *Tile-R* and (b) auxiliary *Tile-R*.

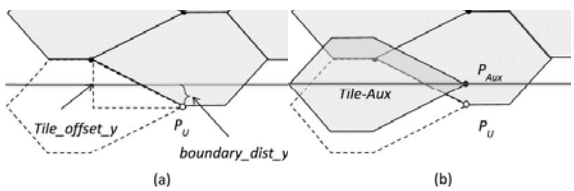

Figure 8. Coverage hole at the lower boundary (Case 4): (a) un-deployed *Tile-L* and (b) auxiliary *Tile-L*.

Case 4 (The hole appears at Row_{2r+1}): In this case, the hole is caused by unable to deploy a *Tile-L* at location $P_U = (x_U, y_U) = (d(v_{T2}, v_{T3}) + Tile\_offset\_x + l \times Tile\_interval\_x, width - (2r+1) \times Tile\_offset\_y)$, where $0 \leq l \leq (j-1)$ and $y_U < 0$. The hole surrounding the lower boundary will look like the one shown in Fig. 8a. The sensing coverage hole can be fully covered by deploying an auxiliary *Tile-L* at $P_{Aux} = (x_U, 0)$ and the connectivity of the WSN is preserved as shown in Fig. 8b.

2) Reduce Sensing Coverage Holes Surrounding the Obstacles

The sensing coverage holes surrounding the obstacles are caused by two reasons: 1) a sensor node deployed at location P_B is blocked by an obstacle; 2) unable to deploy a sensor node at location P_U within an obstacle. We can regard P_B and P_U as locations outside of the deployment area and use the similar approaches proposed in the previous section to fill these coverage holes. After deploying each auxiliary *Tile-L*/*R*, we check if all grid points within the coverage hole are covered. If there are still uncovered grid points, a heuristic algorithm, *Fill-Hole*, illustrated in Fig. 9, will be applied. It first recodes all uncovered grid points, then, for each uncovered grid point *g*, we put a temporary sensor node at *g* and rotate it to find the highest sensing coverage gains (line 5-10). At last, a grid point with the most sensing coverage gains among all grid points is the location of new sensor node (line 13). The process is repeated until all coverage holes are filled or no more sensor nodes can be deployed.

IV. SIMULATION RESULTS

To evaluate the tiling-based WSN deployment under the polygon model, we present some simulation results based on different types of sensor nodes and deployment areas. The sensing area of each type of sensor node is represented by the sector model and the proposed polygon model and two tiling-based deployment approaches under the sector model and the polygon model are applied, respectively. We compare the deployment results of two approaches based on the sensing coverage rate and the usage of sensor nodes.

```
Algorithm Fill-Hole
 1. Scan all uncovered grid points and save to Uncover[];
 2. Let Area be the area of Tile-R/L deployed at P_B or P_U, calculate the current sensing
    coverage rate of Area and save to cov_orig;
 3. while (Uncover[] is not empty and have deployable sensor node){
 4.    for (each grid point g within Uncover[]){
 5.       for (θ_rot from 0° to 360° with step 1°){
 6.          Deploy a new sensor node S_new at g with rotation angle θ_rot;
 7.          Calculate the sensing coverage rate of Area and save to cov_new;
 8.          Save the largest (cov_new - cov_orig) and corresponding θ_rot to score_new and
    rot_new;
 9.          Remove S_new;
 10.      }
 11.      Save score_new and rot_new to Score[] and Rot[];
 12.   }
 13.   Find the index idx of Score[] with the highest score, deploy a new sensor node at
    Uncover[idx] with rotation angle Rot[idx];
 14.   Clear Uncover[] and scan all uncovered grid points and save to Uncover[];
 15.   Calculate the current sensing coverage rate of Area and save to cov_orig;
 16.}
End_of_Fill-Hole
```

Figure 9. The *Fill-Hole* algorithm.

The sensor nodes used in the simulation are composed of an omnidirectional antenna and a directional sensor. We use three types of directional sensors with different shapes of sensing areas and denote them as *Type A*, *Type B*, and *Type C*. Table I shows the actual sensing areas of these sensors and the detailed modeling information, the limit of deployable sensor nodes for each type is set to 1000. To study how the ratio of the maximum communication range to the maximum sensing range (R_C/R_S) influences the deployment results, we use 4 different maximal communication ranges, 80 ($R_C/R_S = 2$), 60 ($R_C/R_S = 1.5$), 40 ($R_C/R_S = 1$), and 30 ($R_C/R_S = 0.75$), for the sensor nodes. To evaluate the influence of the obstacles within the deployment area, three types of the deployment areas, *Area 1*, *Area 2*, and *Area 3*, shown in Fig. 10 are used. The size of each deployment area is 500×500 units. A sink node has one omnidirectional antenna with $R_C = 60$ units is deployed at (150, 150). After the deployment simulation is completed, we calculate the sensing coverage rate based on the actual sensing areas of the deployed sensor nodes. In the following, we describe the simulation results in details based on the type of sensor used by the sensor nodes.

TABLE I. THREE TYPES OF SENSORS USED IN THE SIMULATION

Type A		
Actual sensing area	***Sector model***	***Polygon model***
	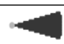	
$R_S = 40$	$sector_S(S_n) = (36.64, 28°)$	$poly_S(S_n) =$ [(40, 0°), (37.59, 11.5°), (32.65, 18.5°), (23.74, 21°), (0, 180°), (23.74, 339°), (32.65, 341.5°), (37.59.5°)]
Type B		
Actual sensing area	***Sector model***	***Polygon model***
		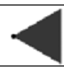
$R_S = 40$	$sector_S(S_n) = (40, 60°)$	$poly_S(S_n) =$ [(46.19, 30°), (0, 180°), (46.19, 330°)]
Type C		
Actual sensing area	***Sector model***	***Polygon model***
		
$R_S = 40$	$sector_S(S_n) = (40, 90°)$	$poly_S(S_n) =$ [(40, 0°), (40, 5°), (40, 15°), (40, 25°), (40, 35°), (40, 45°), (0, 180°), (40, 315°), (40, 325°), (40, 335°), (40, 345°), (40, 355°)]

(a) (b) (c)

Figure 10. Deployment area: (a) Area 1, (b) Area 2, and (c) Area 3.

TABLE II. SIMULATION RESULTS

R_C / R_S	Case 1				Case 2				Case 3			
	Sector-SDP		Polygon-Tiling		Sector-SDP		Polygon-Tiling		Sector-SDP		Polygon-Tiling	
	coverage	#node	coverage	#node	coverage	#node	coverage	#node	coverage	#node	coverage	#node
Area 1												
2	0.9825	783	1	600	0.9675	419	1	404	0.9854	220	1	241
1.5	0.9825	783	1	600	0.9675	419	1	404	0.9854	220	1	241
1	0.9825	783	1	600	0.9675	419	1	404	0.9854	220	1	241
0.75	0.9719	794	1	600	0.9674	425	1	420	0.9655	276	1	300
Area 2												
2	0.8737	459	1	513	0.8064	244	1	386	0.8324	137	1	234
1.5	0.8737	459	1	513	0.8064	244	1	386	0.8324	137	1	234
1	0.8737	459	1	513	0.8064	244	1	386	0.8324	137	1	234
0.75	0.8581	472	1	475	0.8277	250	1	377	0.8090	159	1	285
Area 3												
2	0.9188	500	1	508	0.8880	273	1	426	0.8603	142	1	240
1.5	0.9188	500	1	508	0.8880	273	1	426	0.8603	142	1	240
1	0.9188	500	1	508	0.8880	273	1	426	0.8603	142	1	240
0.75	0.9119	515	1	523	0.8913	275	1	403	0.9070	182	1	285

Regarding to the maximum sensing coverage rate, for *Area 1* without obstacles, the proposed tiling-based deployment approach under the polygon model can produce full sensing coverage rate with optimization while the SDP approach under the sector model cannot. The reason is that the sector model based deployment approach cannot deal with the boundaries of the deployment area and some sensing coverage holes are produced around the boundaries. For deployment areas with obstacles (*Area 2* and *Area 3*), the optimized polygon model based approach still can reach 100% sensing coverage rate. The sector model based approach produces lower sensing coverage rate since no auxiliary tiles used in the polygon model based approach can be deployed around the obstacles. For sensor nodes with $R_C/R_S \geq 1$, we have the same sensing coverage rate in all results. It indicates that the generated tiles for sensor nodes with $R_C/R_S \geq 1$ are identical. Regarding to the usage of sensor nodes, for sensor nodes with $R_C/R_S < 1$, a smaller tile is generated to maintain the network connectivity that increases the usage of sensor nodes.

V. CONCLUSION

In this paper, we have presented the polygon-based sensor modeling and the corresponding tiling-based WSN deployment approach. The proposed polygon model can be used to approximate arbitrary shapes of the directional sensing areas of sensor nodes. The tiling-based WSN deployment under the polygon model can generate a tile with specified number of edges from a given polygon model and use the generated tile to fill the deployment area and maintain the network connectivity. According to the simulation results, the proposed deployment approach can reach full sensing coverage under different types of sensor nodes and deployment areas with or without obstacles. For sensor nodes with the same type of sensor, the proposed approach can maintain the network connectivity under various ratios of the maximum communication/sensing ranges. In addition, the usage of sensor nodes is affected by the area of the generated tile and the intervals between deployed tiles. It is verified that the proposed sensor modeling and tiling-based deployment approach can reach full sensing coverage and maintain network connectivity as compared to the existed sector model based approach in various deployment scenarios.

REFERENCES

[1] N. Ahmed, S. S. Kanhere, and S. Jha, "The holes problem in wireless sensor networks: a survey," *SIGMOBILE Mob. Comput. Commun. Rev.*, vol. 9, no. 2, pp. 4-18, 2005.

[2] J. Ai and A. A. Abouzeid, "Coverage by directional sensors in randomly deployed wireless sensor networks," *Journal of Combinatorial Optimization*, vol. 11, pp. 21-41, 2006.

[3] M. Cardei and J. Wu, "Energy-efficient coverage problems in wireless ad-hoc sensor networks," *Computer Communications*, vol. 29, no. 4, pp. 413-420, 2006.

[4] C. Fulton, "Tessellations," *The American Mathematical Monthly*, vol. 99, no. 5, pp. 442-445, 1992.

[5] A. Ghosh and S. K. Das, "Coverage and connectivity issues in wireless sensor networks: A survey," *Pervasive and Mobile Computing*, vol. 4, no. 3, pp. 303-334, 2008.

[6] B. Grunbaum and G. C. Shephard, "Tilings by Regular Polygons," *Mathematics Magazine*, vol. 50, no. 5, pp. 227-247, 1977.

[7] X. Han, X. Cao, E. L. Lloyd, and C.-C. Shen, "Deploying Directional Sensor Networks with Guaranteed Connectivity and Coverage," in *Proc. 5th Annual IEEE Communications Society Conference on Sensor, Mesh and Ad Hoc Communications and Networks SECON '08*, pp. 153-160, 2008.

[8] H. Ma and Y. Liu, "Some problems of directional sensor networks," *International Journal of Sensor Networks*, vol. 2, no. 1/2, pp. 44-52, 2007.

[9] I. Niven, "Convex Polygons that Cannot Tile the Plane," *The American Mathematical Monthly*, vol. 85, no. 10, pp. 785-792, 1978.

[10] C.-H. Wu and Y.-C. Chung, "A Polygon Model for Wireless Sensor Network Deployment with Directional Sensing Areas," *Sensors*, vol. 9, no. 12, pp. 9998-10022, 2009.